

Semileptonic Decays on the D Meson

W. Bacino, T. Ferguson,^(a) L. Nodulman,^(b) W. Slater, and H. Ticho
Physics Department, University of California, Los Angeles, California 90024

and

A. Diamant-Berger,^(c) G. Donaldson, M. Duro, A. Hall,^(d) G. Irwin, J. Kirkby,
 F. Merritt, and S. Wojcicki
Stanford Linear Accelerator Center and Physics Department, Stanford University, Stanford, California 94305

and

R. Burns,^(e) P. Condon,^(f) and P. Cowell^(g)
Physics Department, University of California, Irvine, California 92664

and

J. Kirz
Physics Department, State University of New York, Stony Brook, New York 11794
 (Received 28 June 1979)

The electron energy spectrum in the process $e^+e^- \rightarrow \psi''(3770) \rightarrow e^\pm + (\geq 2 \text{ charged particles})$ has been used to determine the $D(56\% D^0 + 44\% D^+)$ semileptonic branching ratio. Assuming the Glashow-Iliopoulos-Maiani model, it is found that the inclusive branching ratio is $b(D \rightarrow X e \nu) = 0.080 \pm 0.015$ and the state X is dominated by K and $K\pi$. The fraction of $K\pi e \nu$ is $(37 \pm 16)\%$ if the $K\pi$ system is entirely $K^*(890)$, or $(55 \pm 21)\%$ if the $K\pi$ system is nonresonant. Within the assumptions of the analysis, the D lifetime is calculated to be $(2.5 \pm 1.6) \times 10^{-13}$ sec.

We have studied the final states in the semileptonic decays of D mesons by means of the electron energy spectrum observed in e^+e^- annihilations.¹ The analysis assumes the decays are predominantly $D \rightarrow K(n\pi)e\nu$, $n \geq 0$, following the Glashow-Iliopoulos-Maiani² (GIM) model. The value of the inclusive semileptonic branching ratio measures the strength of the nonleptonic enhancement analogous to that observed in K decays. Furthermore, since the rate $\Gamma(D \rightarrow K e \nu)$ can be reliably calculated,³ the lifetimes of the D^0 and D^+ can be determined from their $K e \nu$ branching ratios. Additional interest in these decay modes arises from the quantum chromodynamics (QCD) calculation of the mass and lifetime of the charmed quark, which uses the measured lepton momentum spectrum and $b(D \rightarrow X e \nu)$.⁴

The data, recorded by the DELCO detector⁵ at SPEAR, is taken from the $\psi''(3770)$ region, $3.76 < E_{c.m.} < 3.78$ GeV. This facilitates our analysis for several reasons: The charm cross section is resonant and therefore can be well measured; the charmed particles are produced simply in $D\bar{D}$ pairs (the $D^0\bar{D}^0:D^+D^-$ ratio is 0.56:0.44 according to phase space) with a known, small velocity ($|P_D| \sim 0.26$ GeV/c). Therefore, the measurements suffer neither from uncertainties in the $c \rightarrow D$ fragmentation nor from substantial Lorentz smearing.

For the purpose of this analysis, we select events with ≥ 3 observed charged particles of which one and only one is identified as an electron by having in-time Cherenkov and shower counter pulses. The minimum pulse heights correspond to 0.07 photoelectron for the Cherenkov counter and 0.3 minimum-ionizing particle for the shower counter. The candidate electron track is required to have at least one hit in the two innermost cylindrical proportional chambers in order to decrease photon conversion backgrounds. To achieve unambiguous electron identification, we retain those events where only one track enters the triggered Cherenkov cell. A further requirement of at least one hit in the outer spark chambers (azimuthal view) ensures a momentum measurement accuracy of $\sigma_p/P = [(0.052)^2 + (0.080P)^2]^{1/2}$, where P is the track momentum in GeV/c.

The electron momentum spectrum of the 596 events which satisfy these criteria is shown in Fig. 1. These data are not yet corrected for backgrounds or Cherenkov detection efficiency (Fig. 2). The predominant background source of high-energy electrons is electronic τ decays⁶ (indicated by the solid line in Fig. 1). The remaining backgrounds come from two sources: hadronic events and two-photon processes. Our studies indicate that the former consists largely of acci-

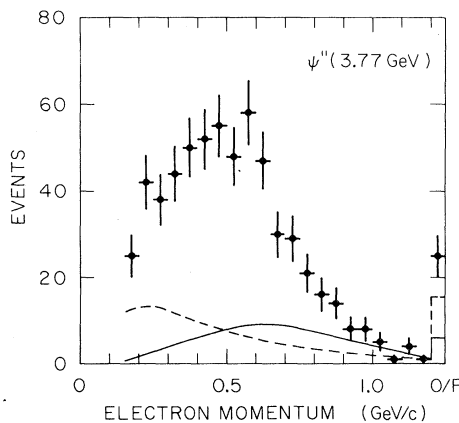


FIG. 1. The electron momentum spectrum from multiprong events observed in the center-of-mass energy range $3.76 < E_{c.m.} < 3.78$ GeV. The solid curve indicates the predicted contribution from τ decays (19% of the observed events). The dashed curve shows all other sources of background (24%).

dental coincidences of a hadronic track and a Cherenkov pulse, either from phototube dark current or γ conversions in the Cherenkov entrance (64% of the hadronic background). Other sources include γ conversions in the beam pipe (15%), electrons from unidentified Dalitz pairs (12%), δ -ray production in the Cherenkov counter (4%), K decays (2%), and Compton scattering (2%). These spectra have been calculated separately and the combined shape and magnitude are compared with the electron spectrum observed in multiprong events at the $\psi(3100)$ [Fig. 3(a)]. The discrepancy between the observed and predicted low-energy electron spectra introduces a small systematic uncertainty which has been included in our final quoted errors. The overall probability for a track to be improperly identified as a candidate electron is about 2×10^{-3} . At energies other than the $\psi(3100)$ and $\psi'(3685)$, several quantum electrodynamics (QED) processes lead to additional electron backgrounds. Calculations of the two-photon final states,⁷ e^+e^-X ($X = \mu^+\mu^-$, $\pi^+\pi^-$, η , η'), and ρ photoproduction,⁸ $e^+e^- \rightarrow e^+e^-\rho$, indicate a contribution of magnitude 0.14 relative to the background from hadronic events. The predicted background in the range $3.50 < E_{c.m.} < 3.52$ GeV [Fig. 3(b)] includes these QED calculations. The level of agreement of the background predictions with the data below charm threshold is a measure of the quality of similar calculations applied to the data of Fig. 1 (indicated by the dashed curve).

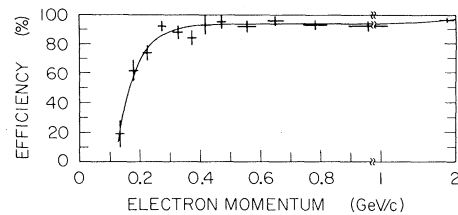


FIG. 2. The Cherenkov-counter detection efficiency vs electron momentum. The curve is drawn through the data points obtained from the final states e^+e^- , $e^+e^-\gamma$, and $e^+e^-e^+e^-$. The efficiency includes geometrical losses due to mirror edges.

After subtracting the backgrounds and correcting for the Cherenkov detection efficiency, we obtain the electron energy spectrum from D decays (Fig. 4). This spectrum can be compared with several hypotheses for D semileptonic decays.⁹ As seen from Fig. 4(a), the spectrum is incompatible with a single decay mode, whether it be $D \rightarrow \pi e \nu$, $D \rightarrow K e \nu$,¹⁰ or $D \rightarrow K^*(890) e \nu$. However, the observed spectrum agrees well with a mixture of these decay modes [Fig. 4(b)]. In this fit we include a contribution from $\pi e \nu$ [with a fixed fraction of $2.0 \tan^2 \theta_C = 0.11$ (Ref. 11) relative to $K e \nu$], since it is the only Cabibbo-suppressed mode whose electron spectrum could

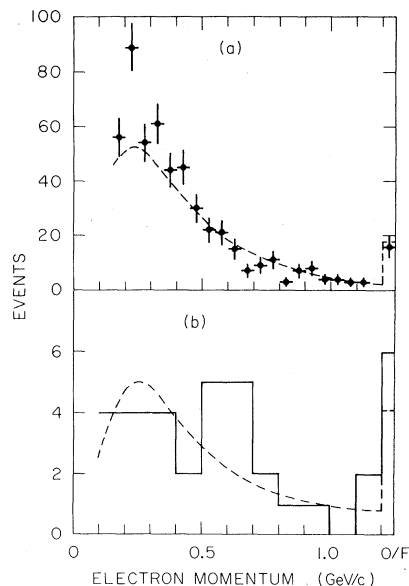


FIG. 3. (a) The electron momentum spectrum from multiprong events observed at the $\psi(3100)$. (b) The electron momentum spectrum observed in the energy range $3.50 < E_{c.m.} < 3.52$ GeV. In both figures the dashed curve shows the predicted spectrum.

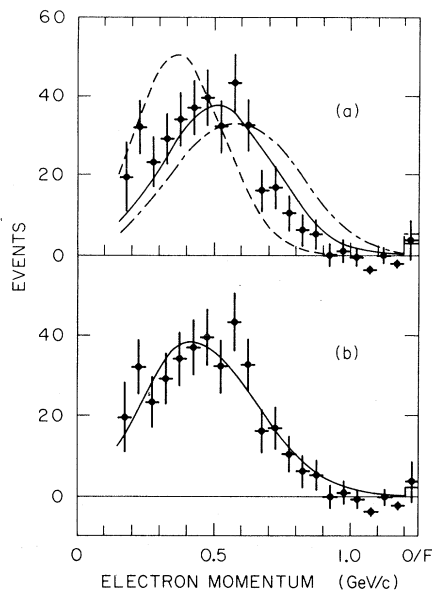


FIG. 4. The electron momentum spectrum from D decays at the ψ' (3770). The curves have been fitted to the data below 1 GeV/c and correspond to the following hypotheses: (a) $D \rightarrow \pi e \nu$ (dot-dashed curve, χ^2 per degree of freedom 80.9/16), $D \rightarrow K e \nu$ (solid curve, χ^2 per degree of freedom 23.4/16), $D \rightarrow K^*(890) e \nu$ (dashed curve, χ^2 per degree of freedom 53.8/16). (b) Contributions from $D \rightarrow K e \nu$ (55%), $D \rightarrow K^*(890) e \nu$ (39%), and $D \rightarrow \pi e \nu$ (6%) (χ^2 per degree of freedom 11.2/15).

bias our results. After accounting for detection efficiencies and systematic errors, we measure¹² the contributions $(37 \pm 16)\%$ ¹³ and $(55 \pm 14)\%$ from $K^*(890)e\nu$ and $Ke\nu$, respectively. This result is insensitive to the $\pi e \nu$ fraction but depends on the assumption of resonant $K\pi$ production. A fit finds contributions of $(55 \pm 21)\%$ and $(38 \pm 19)\%$ from non-resonant $K\pi e \nu$ and $Ke\nu$, respectively,¹⁴ with a χ^2 per degree of freedom of 8.4/15. The systematic uncertainties arising from the background subtraction are determined by varying the individual contributions while retaining compatibility with the data of Fig. 3 and with the experimental values of the τ parameters.

The inclusive electronic branching ratio is determined from the background-subtracted events with use of a Monte Carlo technique to calculate the detection efficiency. This efficiency is insensitive to the relative rates of the π , K , and $K\pi$ semileptonic modes for equal D^+ and D^0 contributions. After accounting for systematic errors, we obtain¹⁵ $b(D \rightarrow Xe\nu) = 0.080 \pm 0.015$.

We have investigated the possible contribution

of $D \rightarrow K\pi\pi e \nu$ by fitting the electron energy spectrum with this channel and varying fractions of $Ke\nu$, $K^*e\nu$, and $K\pi e \nu$. In all fits the $K\pi\pi e \nu$ contribution is small [the largest value is $(11.1^{+20}_{-11})\%$ of the total]. This fraction corresponds to non-resonant $K\pi\pi$ production; it decreases in the case of resonant production such as $Q(1280)$ and $K^{**}(1420)$. In view of this small value it is unlikely that the decays $D \rightarrow K(n\pi)e\nu$, $n \geq 2$, constitute a significant fraction of the D semileptonic decays.

The measured value for $b(D \rightarrow Xe\nu)$, when compared with the naive free-quark estimate of 0.20, suggests that the hadronic decay enhancement is weaker in charm-changing decays than in strange-particle decays. However, we stress that our measurement gives the average semileptonic branching ratios for an approximately equal sample of D^+D^- and $D^0\bar{D}^0$ events and thus does not address itself to the question of equality of the D^+ and D^0 hadronic decay rates.¹⁶ The fact that the D semileptonic decays are dominated by the channels $Ke\nu$ and $K\pi e \nu$ is in reasonable accord with theoretical expectations³ based on the GIM model. The calculations for $\Gamma(D \rightarrow Ke\nu)$ predict $1.4 \times 10^{11} \text{ sec}^{-1}$, assuming F^* dominance of the form factor, or $1.1 \times 10^{11} \text{ sec}^{-1}$ in the case of a constant form factor. Using the former value, we compute the D lifetime to be $(2.5 \pm 1.6) \times 10^{-13} \text{ sec}$, assuming equality of the D^+ and D^0 total decay rates. This value agrees with recent QCD calculations which assume that the lifetime of charmed hadrons is simply the charmed-quark lifetime. This type of calculation is sensitive to the mass of the charmed quark. The authors of Ref. 4 found this mass to lie in range $1.6 < m_c < 1.8 \text{ GeV}/c^2$, using a preliminary version of these electron data.

We acknowledge the invaluable services of the Experimental Facilities Division, SPEAR Operations Group, and Stanford Linear Accelerator Computing Center. This work was supported in part by the U. S. National Science Foundation, and by the U. S. Department of Energy under Contract No. DE-ACD3076F00515.

(a) Current address: Cornell University, Ithaca, N. Y. 14853.

(b) Current address: Argonne National Laboratory, Argonne, Ill. 60439.

(c) Permanent address: Département de Physique de Particules Élémentaires, Saclay, France.

^(d)Current address: Varian Associates, Palo Alto, Cal. 94303.

^(e)Current address: Hughes Aircraft Co., Newport Beach, Cal. 92663.

^(f)Current address: Lawrence Berkeley Laboratory, Berkeley, Cal. 94720.

^(g)Current address: Systems Control, Inc., Palo Alto, Cal. 94303.

¹See R. Brandelik *et al.*, Phys. Lett. **70B**, 387 (1977), and J. M. Feller *et al.*, Phys. Rev. Lett. **40**, 274 (1978), for the results on this subject from the double arm spectrometer at DESY and the Pb Glass Wall experiment, respectively.

²S. L. Glashow, J. Iliopoulos, and L. Maiani, Phys. Rev. D **2**, 1283 (1970).

³M. K. Gaillard, B. W. Lee, and J. L. Rosner, Rev. Mod. Phys. **47**, 277 (1975); J. Ellis, J. K. Gaillard, and D. V. Nanopoulos, Nucl. Phys. **B100**, 313 (1975); A. Ali and T. C. Yang, Phys. Lett. **65B**, 275 (1976); I. Hinchliffe and C. H. Llewellyn-Smith, Nucl. Phys. **B114**, 45 (1976); V. Barger, T. Gottschalk, and R. Phillips, Phys. Rev. D **16**, 746 (1977); W. Wilson, Phys. Rev. D **16**, 742 (1977); F. Bletzacker, M. T. Nieh, and A. Soni, Phys. Rev. D **16**, 732 (1977); D. Fabirov and B. Stech, Nucl. Phys. **B133**, 315 (1978); G. L. Kane, K. Stowe, and W. B. Rolnick, University of Michigan Report No. UM-HE 77-25 (1978) (unpublished).

⁴M. Suzuki, Nucl. Phys. **B145**, 420 (1978); N. Cabibbo and L. Maiani, Phys. Lett. **79B**, 109 (1978); A. Ali and E. Pietarinen, DESY Report No. DESY 79/12, 1979 (unpublished); N. Cabibbo, G. Corbo, and L. Maiani, Rome University Report No. 79-0279, 1979 (unpublished).

⁵W. Bacino *et al.*, Phys. Rev. Lett. **70B**, 387 (1977).

⁶We use the branching ratios $b(\tau \rightarrow e \nu_e \nu_\tau) = 0.16$ and $b(\tau \rightarrow (\geq \text{three charged particles}) \nu_\tau) = 0.26$. In the subsequent error analysis these numbers are given systematic errors of ± 0.03 and ± 0.06 , respectively.

⁷J. Vermaseren, private communication.

⁸Rohini Godbole and J. Smith, CERN Report No. CERN-TH-2648, 1979 (unpublished).

⁹We have derived the theoretical spectra from the papers in Ref. 3 of Wilson and of Ali and Yang (setting the parameter $\delta = 0$). The $Ke\nu$ spectrum includes a form factor dominated by F^* (although the shape is insensitive to this assumption) and the $K^*e\nu$ spectrum assumes a $V-A$ current.

¹⁰Although the $Ke\nu$ fit is acceptable by a χ^2 test, it displays a systematic shift toward high momenta. These point-to-point correlations are measured by an independent statistical parameter known as the "runs test," described by W. T. Eadie *et al.*, *Statistical Methods in Experimental Physics* (North-Holland, Amsterdam and London, 1971). When applied to the $Ke\nu$ fit of Fig. 4(a), it associates a probability of 5×10^{-3} with the hypothesis of pure $D \rightarrow Ke\nu$.

¹¹Bletzacker, Nieh, and Soni, Ref. 3.

¹²This measurement is strongly dependent on the $V-A$ assumption. A $V+A$ current hardens the electron spectrum and gives an acceptable fit with the single decay $D \rightarrow K^*(890)e\nu$.

¹³The calculation of the $K\pi$ fraction involves a small subtraction of the $\pi\pi$ contribution.

¹⁴A fit of the single decay mode $D \rightarrow K\pi e\nu$ has a χ^2 per degree of freedom of 19.8/16 and a "run test" probability of 2×10^{-2} .

¹⁵This measurement of $b(D \rightarrow Xe\nu)$ follows the original Breit-Wigner analysis described in Ref. 5. The new value, which differs from our previous measurement of 0.11 ± 0.02 , results from a larger electron background estimation. In particular, the τ contribution was not included previously, since it was not known that the ψ' mass exceeded $\tau^+\tau^-$ threshold.

¹⁶M. Katuya and Y. Koide, Shizuoka Women's University Report No. SH-78-05, 1978 (unpublished).

¹⁷For a recent discussion of other experimental data bearing on the D lifetime, see S. G. Wojcicki, in SLAC Report No. 215, 1978 (unpublished).